ANNUAL REPORT 2009

UIUC, August 5, 2009

Modeling heat transfer, precipitate formation, and grain growth during secondary spray cooling

Kun Xu

(Ph.D. Student)

Department of Mechanical Science and Engineering

University of Illinois at Urbana-Champaign

Objectives

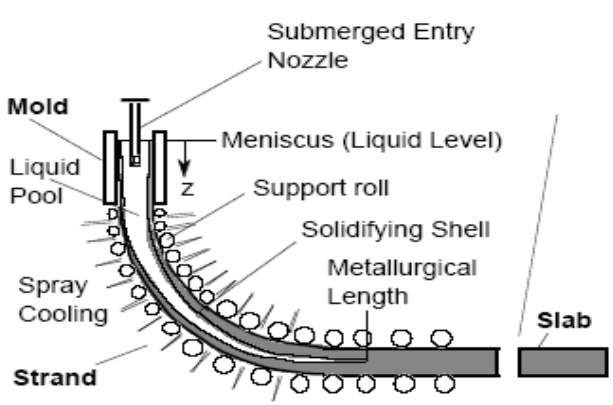

Cracks form during cooling due to:

- tensile stress

- low ductility

➢ To design temperature histories to avoid crack formation, need accurate predictive tools

➢ Models can now accurately predict temperature and stress histories

➢ Need tools to predict metallurgical behavior to estimate hot ductility, such as grain size, precipitate formation

Specific application: transverse surface cracks

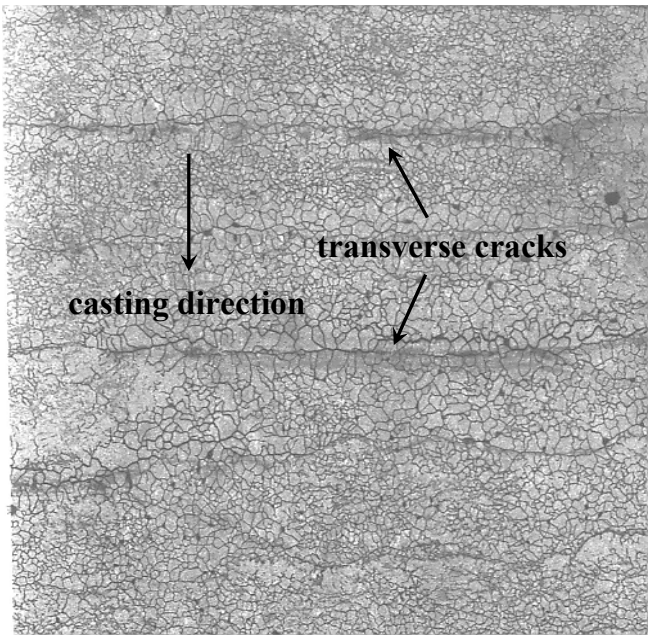

Widespread crazing and fine transverse cracks at oscillation marks on the as-cast surface of a line pipe steel slab (top side)

E. S. Szekeres,Proceedings of the 6th International Conference on Clean Steel, Hungary, 2002.

Effect of depressions on grain size and cracks

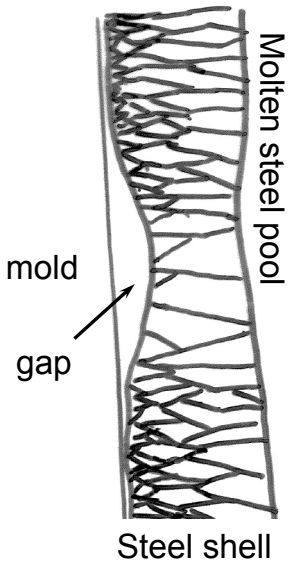

Larger grains and cracks beneath depressions & oscillation marks

Due to:
- More heat flow resistance across gap
- Higher shell temperature
- Faster grain growth

Causes:
- Tensile strain concentration area
- Make hot grains actually align (Secondary recrystallization) to form "blown grains"
- Embrittled with the large numbers of fine precipitates at weak grain boundaries — transverse cracks open up along boundaries

Mechanism of surface crack formation with precipitate embrittlement

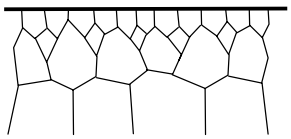

STAGE I - Normal solidification on mold wall. Surface grains are small but highly oriented.

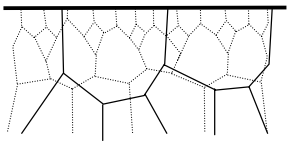

STAGE II - Surface grains "blow" locally due to high temperature (>1350°C) and strain, especially at the base of deeper oscillation marks.

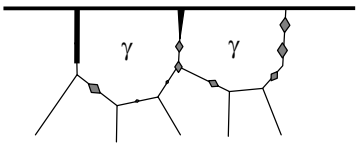

STAGE III - Nitride precipitates begin to form along the blown grain boundaries. Microcracks initiate at weak boundaries.

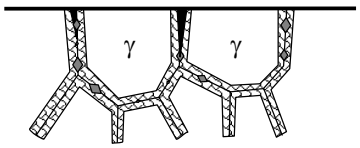

STAGE IV - Ferrite transformation begins and new precipitates form at boundaries. Existing micro-cracks grow & new ones form.

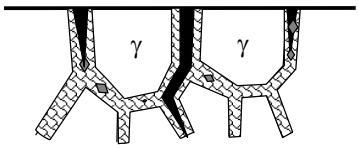

STAGE V - At the straightener, microcracks propagate and become larger cracks, primarily on top surface of the strand.

E. S. Szekeres,Proceedings of the 6th International Conference on Clean Steel, Hungary, 2002.

Cracks open up at weak grain boundaries

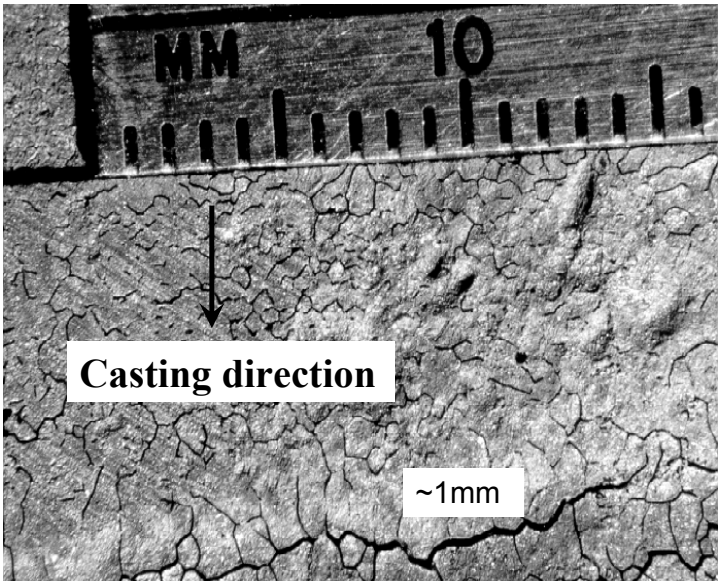

Crazing around a transverse crack at base of an oscillation mark on the as-cast top surface of a 0.2%C steel slab

Note larger grain size (typical size ~1mm) at the base of oscillation mark

E. S. Szekeres,Proceedings of the 6th International Conference on Clean Steel, Hungary, 2002.

Hot ductility varies with temperature and grade due to precipitate formation

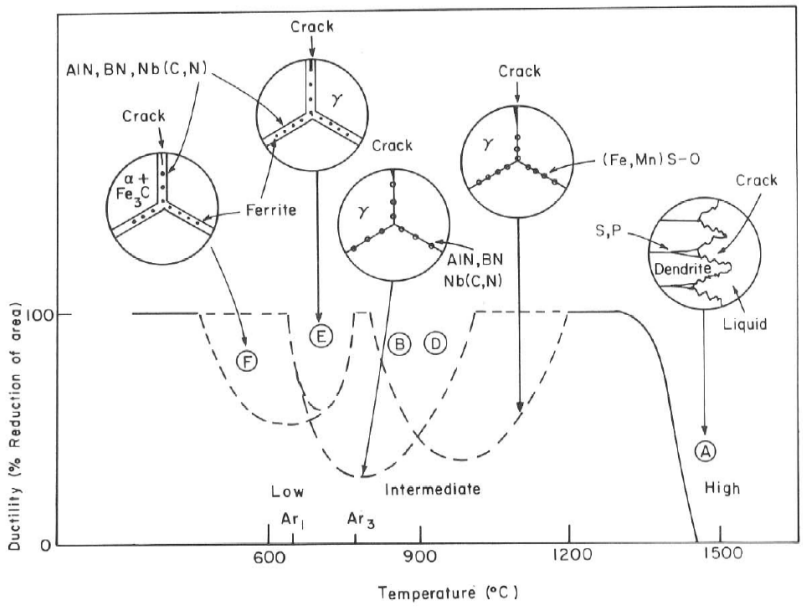

B.G. Thomas et al, ISS Transactions, 1986, 7-20.

Micrographs of precipitates in steels

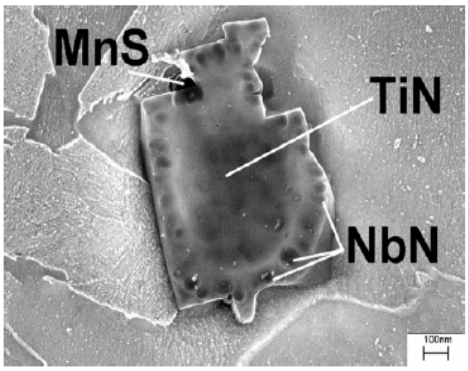

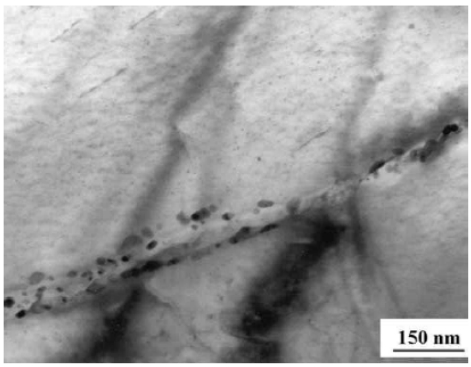

Complex precipitates with TiN core

TiNb(C) precipitates at grain boundaries

V. Ludlow et al, Precipitation of nitrides and carbides during solidification and cooling, unpublished work.

M. Charleux et al, *Metallurgical and Materials Transactions A*, 2001, vol.32A, 1635-1647.

Project Overview

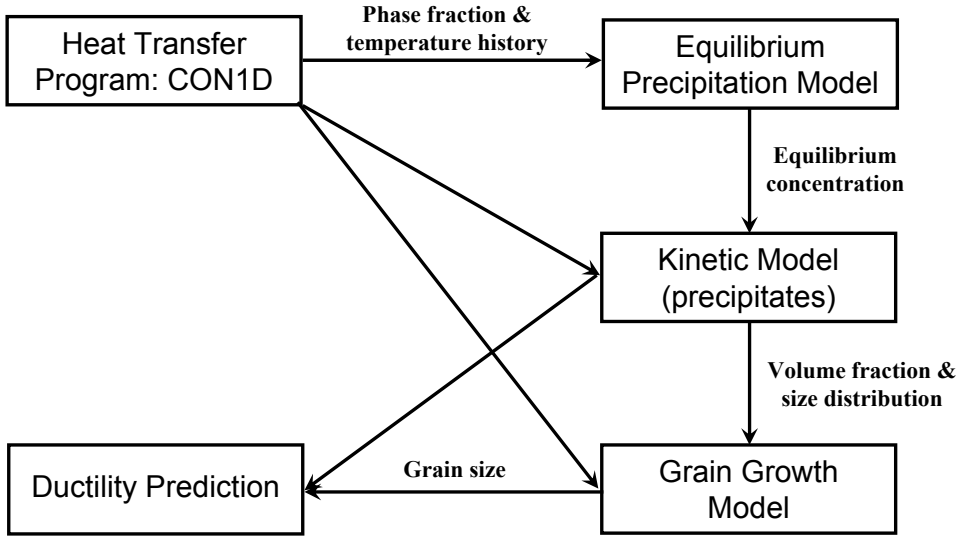

Final goal ⇨ Predict ductility and combine with other models to design casting practices to prevent cracks

Equilibrium precipitation model

Reaction $xM + yX \rightleftarrows M_x X_y$ M: metal, X: C, N, S or O

Solubility product: $K_{M_x X_y} = a_{[M]}^x \cdot a_{[X]}^y / a_{(M_x X_y)}$

$\alpha_{(MxXy)}$: activity of precipitates

$a_i = f_i[\%i]$ where $\log f_i = e_i^i[\%i] + \sum e_i^j[\%j]$

[%i]: dissolved concentration of element i

Mutual Solubility: If two precipitates have the same crystal structures and similar lattice parameters (<10%), they are mutually soluble

For example, NbN and TiN are mutually soluble

$$a_{[Nb]} \bullet a_{[N]} / a_{NbN} = K_{NbN} \qquad a_{[Ti]} \bullet a_{[N]} / a_{TiN} = K_{TiN} \qquad a_{NbN} + a_{TiN} = 1$$

NbN and AlN are mutually exclusive

$$a_{[Nb]} \bullet a_{[N]} = K_{NbN} \qquad a_{[Al]} \bullet a_{[N]} = K_{AlN}$$

System of nonlinear equations include:

1. Solubility limit for each precipitate with consideration of mutual solubility and influence on activities from interaction between elements
2. Mass balance for each element during precipitation
3. Constraints for mutually soluble coefficients

Groups of precipitates

The current model has 18 precipitates, 13 alloying elements and 4 groups of mutually soluble precipitates

- TiN, TiC, NbN, $NbC_{0.87}$, VN, V_4C_3 (**f.c.c structure**) lattice mismatch ~7.92%
  - Validated by many experimental observations
- Al_2O_3, Ti_2O_3 (**hexagonal structure**) lattice mismatch ~8.06%
- MgO, MnO (**f.c.c structure**) lattice mismatch ~5.54%
- MnS, MgS (**f.c.c structure**) lattice mismatch ~0.38%
- SiO_2 (**trigonal structure**)
- TiS (**trigonal structure**)
- $Ti_4C_2S_2$ (**hexagonal structure**)
- AlN (**hexagonal structure**)
- BN (**hexagonal structure**)
- Cr_2N (**hexagonal structure**)

- A complete system of 35 nonlinear equations is solved with Newton-Raphson method

Validation for mutually exclusive precipitates

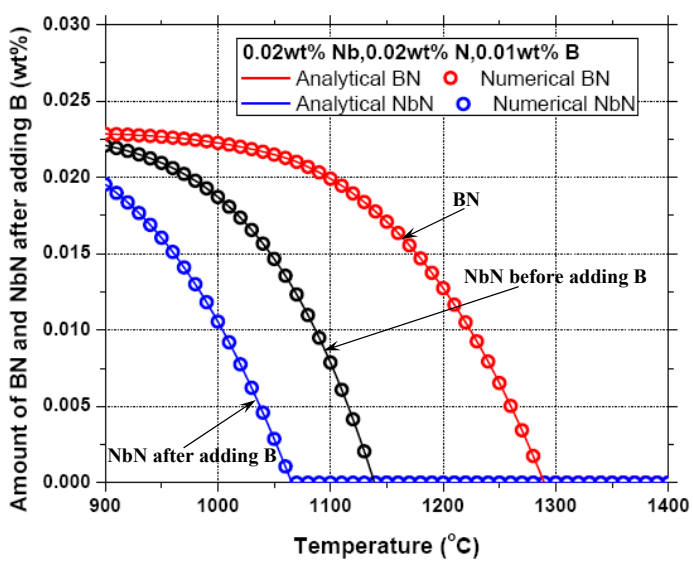

Three hypothetical steels

1. 0.02%Nb and N
2. 0.02%Nb and N, 0.02% Al
3. 0.02%Nb and N, 0.01% B

Second order equation and analytical solution exists

➢ Existing precipitate AlN or BN delays the precipitate NbN to form at the lower temperature and decreases the equilibrium amount of NbN at the same temperature

Pseudo-ternary diagram for Al-Nb-N system

Fix the sum of weight percent concentration (Al+Nb+N) as 0.05%

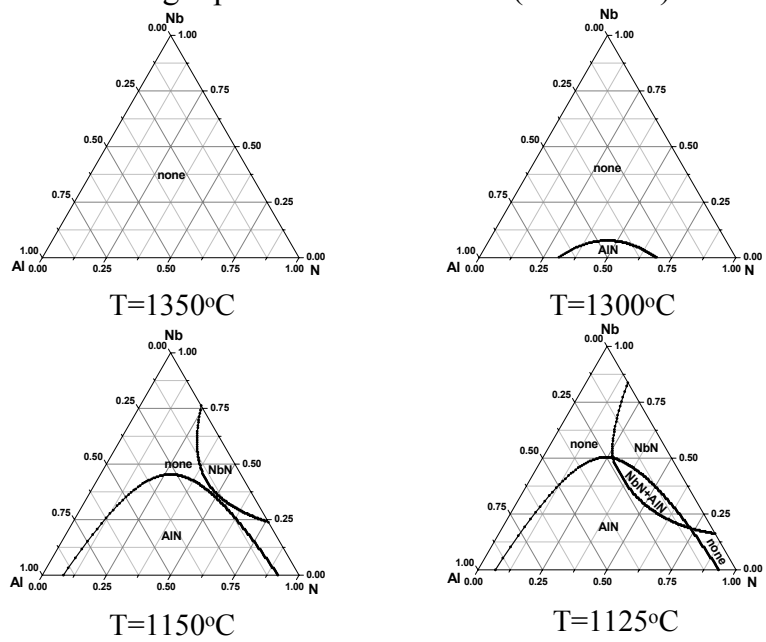

Test problem for mutually solubility (Ti-Nb-N system)

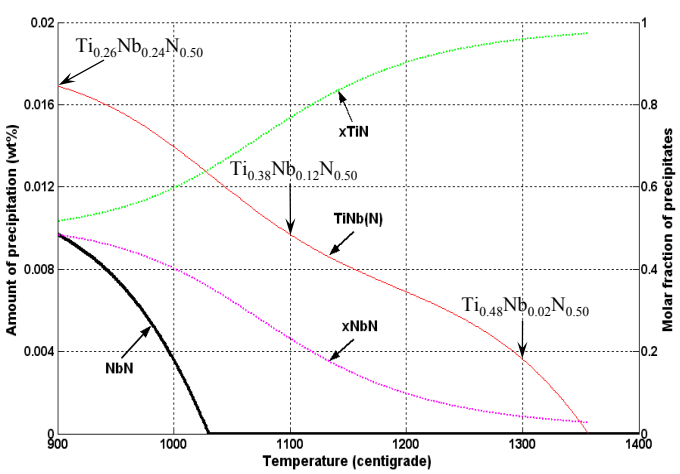

Three hypothetical steels
1. 0.01%Nb and N
2. 0.01%Nb and N, 0.005% Ti

At least fourth order equation and no analytical solution

- Mutual solubility decreases the activity of NbN, which allows more NbN to form
- Without consideration of mutual solubility, NbN precipitates would decrease with Ti additions

Validation with stability of TiS and $Ti_4C_2S_2$

Steel	C	Si	Mn	S	Al	Ti	N	O
B	0.0036	0.0050	0.081	0.0028	0.045	0.095	0.0019	0.0028
C	0.0033	0.0040	0.081	0.0115	0.037	0.050	0.0022	0.0036

Recorded types of observed precipitates in experiments (matches prediction)

Measurements: X. Yang et al, *ISIJ International*, 1996, vol.36, 1286-1294.

Steel	1300°C	1250°C	1200°C	1150°C	1100°C
B	TiN	TiN, TiS*	TiN, TiS	TiN, $Ti_4C_2S_2$	TiN, $Ti_4C_2S_2$
C	TiN, TiS	TiN, TiS	TiN, TiS	TiN, TiS	TiN, TiS*, $Ti_4C_2S_2$

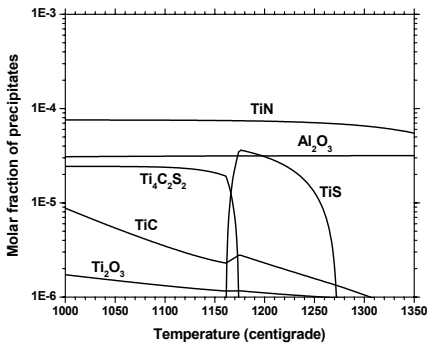

Steel B

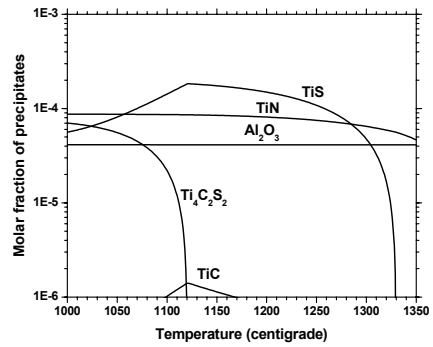

Steel C

Validation with equilibrium Nb(C,N) precipitation experiments (microalloy steel)

Steel	C	Si	Mn	P	S	Nb	Al	N	V	Ti
Nb1	0.085	0.28	1.46	0.008	0.002	0.013	0.013	0.005	0.014	0.003
Nb8	0.081	0.31	1.44	0.01	0.002	0.033	0.017	0.004	0.011	0.003

Measurements: S. Zajac and B. Jansson, *Metallurgical and Materials Transactions B*, 1998, vol.29B, 163-176.

Solution treated (1300°C) 1 hour

Followed by water quenching

Then aged at different isothermal temperature for 24-48 hours

Cool to ambient quickly

Measure Nb amount in Nb(C,N) by the inductively coupled plasma (ICP) emission method

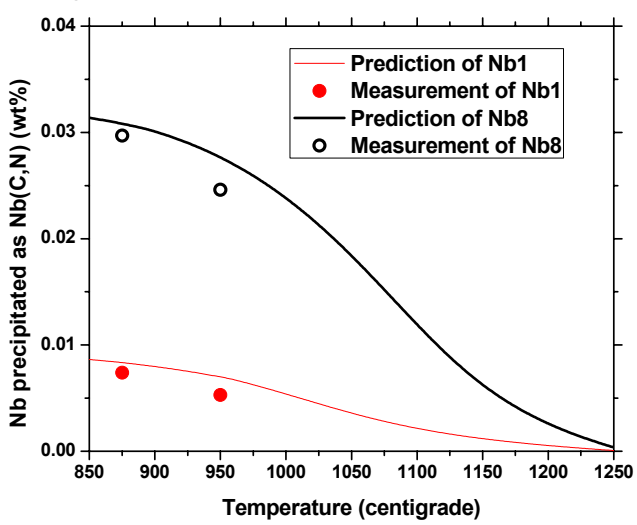

Temperature and steel phase fraction model

CON1D Program: Solve the transient heat conduction in the mold and spray regions of continuous steel slab casters using finite difference method

The program is calibrated to predict the temperature of the real casters.

Example: thin slab casting of low-carbon 1006N2 steel

Steel	C	N	S	Mn	Si	Ti	Nb	V	Al	B	Cr
1006N2	0.0472	0.0083	0.0013	0.9737	0.2006	0.0084	0.0123	0.0027	0.0223	0.0001	0.0354

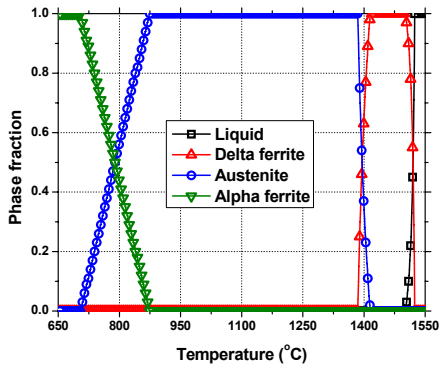

Slab size: 90mm thick, 1396mm wide
Mold length: 950mm
Pouring Temperature: 1553°C
Casting speeds: 2.8m/min and 4.6m/min

Liquidus temperature: 1524.4°C
Solidus temperature: 1500.7°C

Equilibrium Precipitation in continuous casting of 1006N2 Steel

Mold length 0.95m, start of first spray zone 0.85m, end of last spray zone 11.25m

Only precipitates predicted to form are: (Ti,Nb,V)(C,N), MnS and AlN

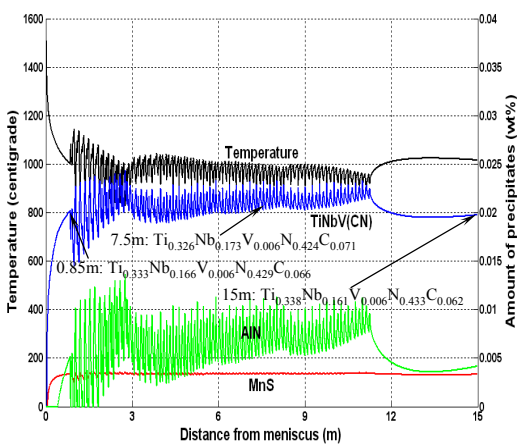

V=2.8m/min

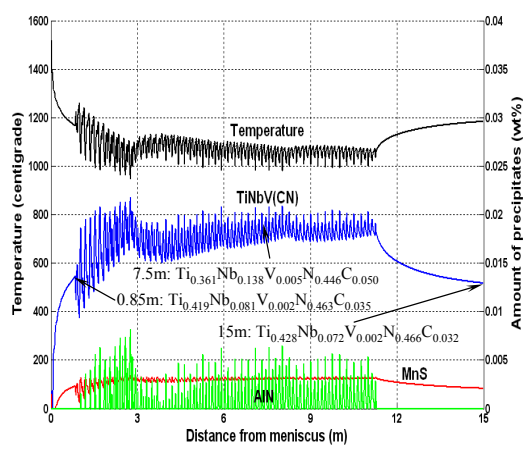

V=4.6m/min

Higher casting speed causes higher temperature and less precipitates (same spray flows)

TiN is most stable at high temperature because of its low solubility limit. For the higher casting speed, AlN does not form in the mold.

Kinetic model for precipitate growth

Particle Collision

$$\frac{dn_i}{dt} = \underbrace{\frac{1}{2}\sum_{k=1}^{i-1}(1+\delta_{k,i-k})\Phi_{k,i-k}n_k n_{i-k}}_{\text{Generation of size i particle by collision of smaller particles k and i-k, only count once for reacting particles}} - \underbrace{n_i\sum_{k=1}^{n_M}(1+\delta_{i,k})\Phi_{i,k}n_k}_{\text{Loss of size i particle by collision with any particle j, double loss if both particle i}} \quad (i \geq 2)$$

Particle Diffusion

$$\frac{dn_i}{dt} = \underbrace{-\beta_i n_1 n_i}_{\text{Particle Diffusion (i→i+1)}} + \underbrace{\beta_{i-1} n_1 n_{i-1}}_{\text{Particle Diffusion (i-1→i)}} \underbrace{-\alpha_i A_i n_i}_{\text{Particle Dissolution (i→i-1)}} + \underbrace{\alpha_{i+1} A_{i+1} n_{i+1}}_{\text{Particle Dissolution (i+1→i)}} \quad (i \geq 2)$$

Collision happens only in liquid, and diffusion happens in both liquid and solid

n_i: Number density of size i particle (m^{-3})

Φ_{ij}: Collision coefficient for collision between size i and size j particle (m^3/s)

β_i: Diffusion rate constant of size i particle (m^3/s) $\beta_i = 4\pi D_1 r_i$

α_i: Dissolution rate per unit area of size i particle ($m^{-2}s^{-1}$) $\alpha_i = \beta_i n_{1,eq} \exp\left(2\sigma V_m / RTr_i\right) / A_i$

Introduction of Particle Size Grouping (PSG) model

- The model always simulates from nuclei (~ 0.1nm) up to large coarsened particles (~100μm): particles could contain $1\sim10^{18}$ molecules
- Serious computation and memory storage issues arise with such a large size range
- Solve with PSG method: Use N_G groups (<100) of geometrically progressing size

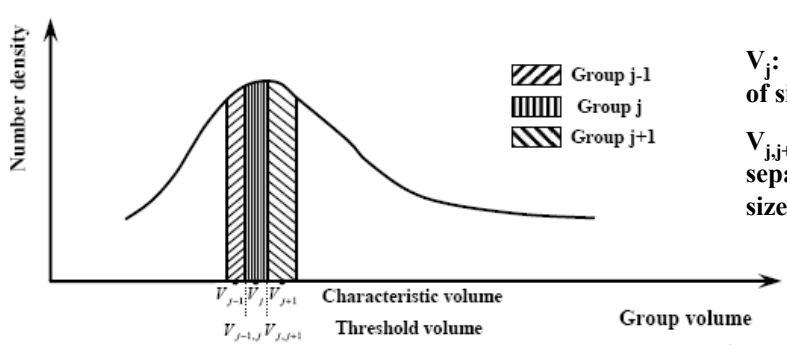

V_j: Characteristic volume of size group j particle

$V_{j,j+1}$: Threshold volume to separate group j and j+1 size group particles

$$V_{j,j+1} = \sqrt{V_j V_{j+1}}$$

Average particle volume ratio

$$R_V = V_{j+1} / V_j$$

Total number density of each size group $N_j = \int_{V_{j-1,j}}^{V_{j,j+1}} n(V)dV$

Size group and particle radius for constant R_V

R_V=2			R_V=3		
Size group	Number of molecules	Particle size	Size group	Number of molecules	Particle size
1	1	0.174nm	1	1	0.174nm
2	2	0.219nm	2	2-5	0.219-0.298nm
3	3-5	0.251-0.298nm	3	6-15	0.316-0.429nm
4	6-11	0.316-0.387nm	4	16-46	0.439-0.624nm
5	12-22	0.398-0.488nm	5	47-140	0.628-0.904nm
6	23-45	0.495-0.619nm	6	141-420	0.906-1.303nm
7	46-90	0.624-0.780nm	7	421-1262	1.304-1.881nm
8	91-181	0.783-0.985nm	8	1263-3787	1.881-2.713nm
9	182-362	0.986-1.240nm	9	3788-11363	2.713-3.913nm
10	363-724	1.242-1.563nm	10	11364-34091	3.913-5.644nm
11	725-1448	1.564-1.969nm	...	...	...
12	1449-2896	1.970-2.481nm	15	2.8×10^{6}-8.3×10^{6}	24.42-35.22nm
13	2897-5792	2.481-3.126nm	20	6.7×10^{8}-2.0×10^{9}	0.152-0.220μm
14	5793-11585	3.126-3.938nm	25	1.6×10^{11}-4.9×10^{11}	0.951-1.371μm
15	11586-23170	3.938-4.962nm	30	4.0×10^{13}-1.2×10^{14}	5.934-8.558μm
...	...	...	35	9.6×10^{15}-2.5×10^{16}	37.03-53.40μm
20	3.7×10^{5}-7.4×10^{5}	12.50-15.75nm	40	2.3×10^{18}-7.0×10^{18}	231.1-333.3μm
25	1.2×10^{7}-2.4×10^{7}	39.70-50.01nm			
30	3.8×10^{8}-7.6×10^{8}	0.126-0.159μm			
35	1.2×10^{10}-2.4×10^{10}	0.400-0.504μm			
40	3.9×10^{11}-7.8×10^{11}	1.270-1.600μm			

* The calculation of particle size is special for AlN with V_m=1.33×10^{-5} m^3/mol

Validation of test problem for collision

Turbulent collision $\Phi_{ij} = 1.3(\varepsilon/\nu)^{1/2}(r_i + r_j)^3$ with only single molecules initially

Dimensionless form $n_i^* = n_i / n_0 \quad t^* = 1.3(\varepsilon/\nu)^{1/2} r_1^3 n_0 t$

n_0: Initial number density of single molecules; ε , ν , r_1 are input parameters

Initial condition (t*=0): n_1^*=1 and n_i^*=0 for i⩾2 (same for N_i in PSG model))

Boundary condition: n_M^*=0, or N_G^*=0 at all t*

Exact solution: n_M=12000; **PSG model**: N_G=16 (R_V=2) or N_G=11 (R_V=3)

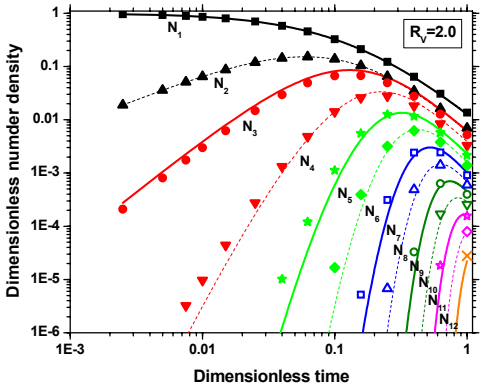

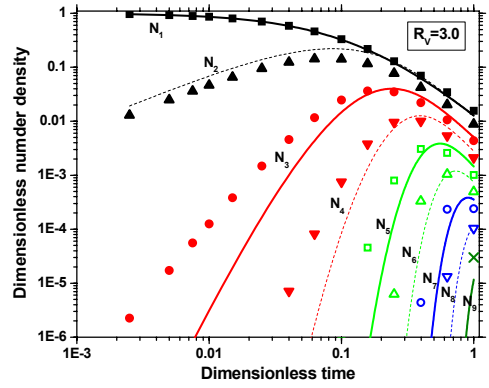

Develop new PSG method for diffusion

$$\frac{dN_j}{dt} = \underbrace{\frac{V_1}{V_j}\beta_j N_1 (N_j - n_j^U)}_{\substack{\textbf{Diffusion}\\ \textbf{inside group j}}} - \underbrace{\frac{V_1}{V_j}\alpha_j A_j (N_j - n_j^L)}_{\substack{\textbf{Dissolution}\\ \textbf{inside group j}}} + \underbrace{\frac{ceil(V_{j-1,j})}{V_j}\beta_{j-1}^U N_1 n_{j-1}^U}_{\substack{\textbf{Diffusion}\\ \textbf{group j-1}\rightarrow\textbf{j}}} + \underbrace{\frac{floor(V_{j,j+1})}{V_j}\alpha_{j+1}^L A_{j+1}^L n_{j+1}^L}_{\substack{\textbf{Dissolution}\\ \textbf{group j+1}\rightarrow\textbf{j}}}$$

$$\underbrace{-\frac{floor(V_{j,j+1})}{V_j}\beta_j^U N_1 n_j^U}_{\substack{\textbf{Diffusion}\\ \textbf{group j}\rightarrow\textbf{j+1}}} \underbrace{-\frac{ceil(V_{j-1,j})}{V_j}\alpha_j^L A_j^L n_j^L}_{\substack{\textbf{Dissolution}\\ \textbf{group j}\rightarrow\textbf{j-1}}} \quad (j \geq 2)$$

n_j^L : Number density of particles in group j, which jumps into group j-1 by dissolution after losing only one single molecule

n_j^U : Number density of particles in group j, which jumps into group j+1 by diffusion after getting only one single molecule

Estimated from geometric progression of the number densities for two neighboring size groups

Validation of test problem for diffusion

Dimensionless form $n_i^* = n_i / n_{1,eq}$ $t^* = 4\pi D_1 r_1 n_{1,eq} t$

Molecules produced by an isothermal first order reaction

$$n_s^*(t^*) = n_s(t^*)/n_{1,eq} = \sum_{i=1}^{n_M} i \cdot n_i^* = 9[1-\exp(-0.1t^*)]$$

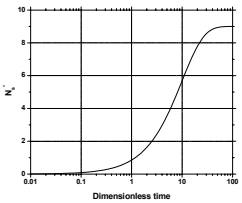

Initial condition (t*=0): $n_i^*=0$ for $i \geqslant 1$ (same for N_i in PSG model)

Boundary condition: $n_M^*=0$, or $N_G^*=0$ at all t*

Exact solution: n_M=16000; **PSG model**: N_G=17 (R_V=2) or N_G=12 (R_V=3)

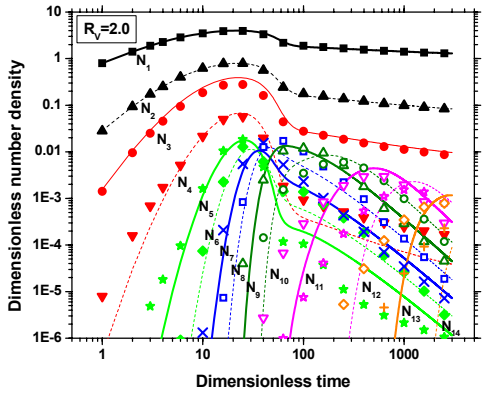

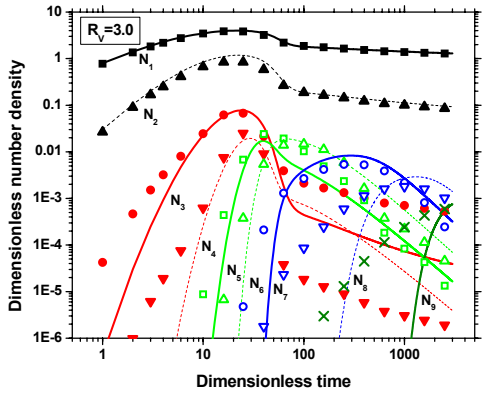

Compare computational cost for test problems

	Collision			Diffusion		
	Exact	PSG (R_v=2)	PSG (R_v=3)	Exact	PSG (R_v=2)	PSG (R_v=3)
Storage	n_M=12000	N_G=16	N_G=11	n_M=16000	N_G=17	N_G=12
Computational time	~225 hours	~0.8s	~0.4s	~7420s	~358s	~248s

* Calculation is run with Matlab on Dell OPTIPLEX GX270 with P4 3.20GHz CPU and 2GB RAM

For constant R_V, the number of size groups in PSG method must satisfy

$$V_{N_G} = R_V^{N_G-1} > n_M \quad \rightarrow \quad N_G = Ceil(\log_{R_V} n_M) + 1 + 1 \text{ (last one for boundary group)}$$

The computational time is proportional to n_M^2 or N_G^2 for collision problem (double loop), and n_M or N_G for diffusion problem (single loop)

Computation cost is dramatically reduced, especially for the problem with a large variety of precipitate sizes because of logarithm relation

Sample results for AlN particles

V_M=1.33×10^{-5}m^3/mol, σ=0.2~0.75J/m^2

D_{Al}=3*10^{-3}exp(-234500/RT) m^2/s, D_N=9.1*10^{-5}exp(-168500/RT) m^2/s

Solubility product in austenite $\log K_{AlN} = -\frac{6770}{T} + 1.03$, Al_0=0.011wt%, N_0=0.009wt%

Choose R_V=2 and 30 size groups, Δt=1×10^{-3}s, Implicit Euler with Gauss-Seidel iterative method

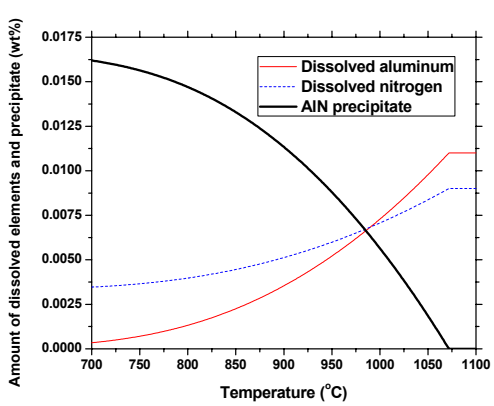

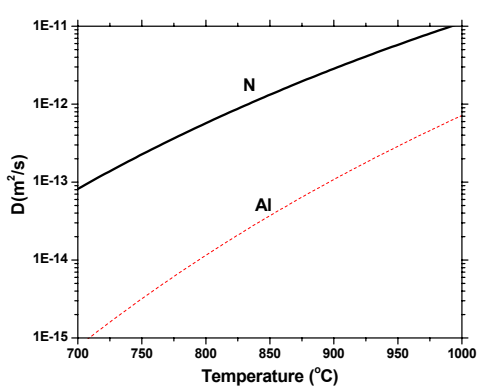

Calculated size distribution

Choose σ=0.5J/m^2

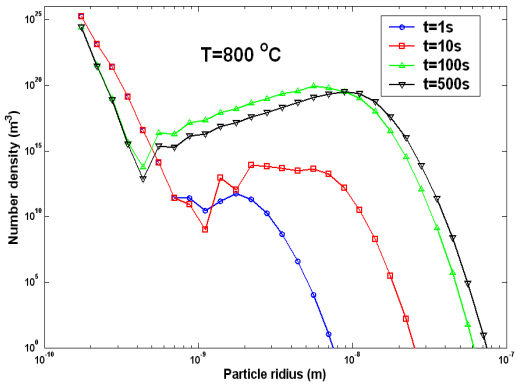

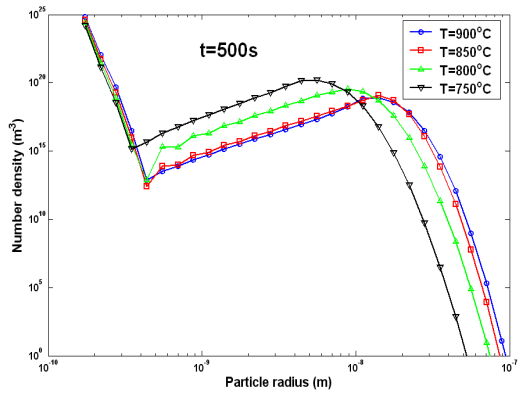

Growth (10~100s) is quick, coarsening (100-500s) is slow

Lower temperature causes higher nucleation rate, thus large number of fine precipitated particles are observed

Generate PTT diagram

$$\Pi = N_1 / N_{1,eq} \qquad f = \frac{N_t / N_{1,eq} - \Pi}{N_t / N_{1,eq} - 1}$$

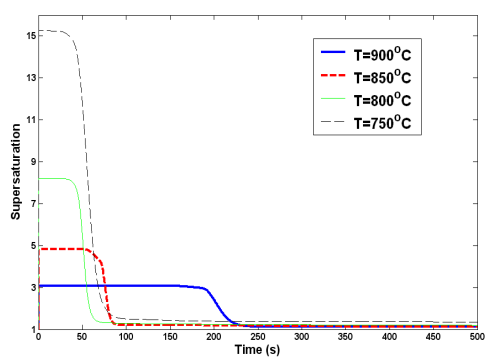

Temperature	5% precipitated	Precipitated (500s)
900°C	178.1s	94.4%
850°C	60.2s	97.0%
800°C	40.3s	97.3%
750°C	38.5s	97.6%

Experimental PTT curves of AlN precipitated in austenite of 0.051%Al-0.0073%N steel

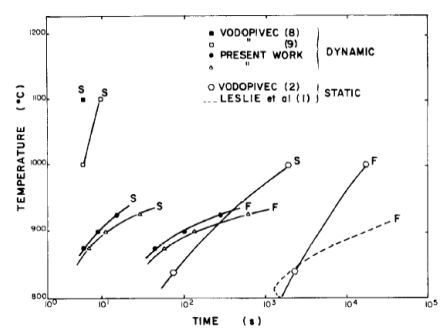

J. P. Michel et al, Acta Metallurgica, 1981, 513-526.

Quicker precipitation and higher nose temperature: interfacial energy value are between 0.5-0.75J/m^2

Grain growth model

Grain growth in austenite under the presence of precipitates

$$\frac{d\bar{D}}{dt} = M_0^* \exp\left(-\frac{Q_{app}}{RT}\right)\left[\frac{1}{\bar{D}} - \frac{1}{k}\frac{f}{r}\right]^{(1/n-1)}$$

M_0*: Kinetic constant that represents grain boundary mobility (m^2/s)

Q_{app}: Apparent activation energy for grain growth (J/mol)

n: Exponent to measure resistance to grain boundary motion

f and r: the volume fraction and radius of precipitates

K: Zener coefficient related to pinning efficiency of the precipitates.

The maximum grain diameter in the presence of precipitates is defines as $\bar{D}_{Lim} = kr/f$

Calculation begins from the temperature of totally austenite structure, the initial austenite grain size is assumed to be with the order of the primary dendrite arm spacing (PDAS)

$\lambda_1 = K\left(C_R\right)^m (C_0)^n$ $K=278.75$, $m=-0.20628$, $n=-0.3162+2.0325C_0$ for $0 \leqslant C_0 \leqslant 0.15$ (wt pct)

I. Andersen and Ø Grong, Acta Metallurgica Materialia, 1995.

M. E. Bealy and B. G. Thomas, Metallurgical and Materials Transactions B, 1996.

Grain growth of 1006N2 steel in continuous casting

Neglect the influence of precipitates

$$\frac{d\bar{D}}{dt} = M_0^* \exp\left(-\frac{Q_{app}}{RT}\right)\left[\frac{1}{\bar{D}} - \cancel{\frac{1}{k}\frac{f}{r}}\right]^{(1/n-1)}$$

$M_0^*=4\times10^{-3}m^2/s$, n=0.5,
Q_{app}=167686+40562(wt%C_p)
wt%C_p=wt%C-0.14wt%Si+0.04wt%Mn

J. Reiter, C. Bernhard and H. Presslinger, MS&T 2006, Cincinnati, USA.

Fully austenite temperature 1384°C

Cooling rate estimated by CON1D

Without precipitates: the grains large enough to cause cracks

Rough estimation: At surface, volume fraction of TiN $1.45*10^{-4}$ at mold exit by choosing ρ_{steel}=7500kg/m^3 and ρ_{TiN}=5420kg/m^3, typical average TiN particle size 10~100nm and k=4/3. the maximum grain size is calculated within the range of 90~900μm

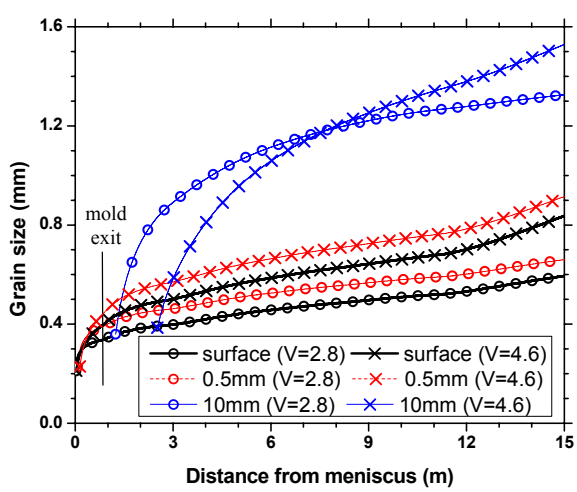

Conclusions (equilibrium precipitation model)

1) An equilibrium precipitation model is established, which includes consideration of solubility limit with Wagner interaction effect, mutual solubility and complete mass conservation of alloying elements.
2) The influence of mutual solubility on precipitation behaviors is carefully considered. Pseudo-ternary precipitation diagram is produced.
3) The model is validated with analytical solutions of simple cases and experimental measurements of literatures. Good agreements are found.
4) The model is applied for practical 100N2 steel and continuous casting with two casting speed. TiNbV(CN), Mns and AlN are only possible precipitates that could form. TiN is the mainly precipitates at high temperature especially in the mold because of its lowest solubility limit. With higher speed, AlN does not form in the mold.

Conclusions (kinetic model)

1) Comparing with some empirical or semi-empirical kinetic precipitation models, the suggested precipitate growth mechanisms by collision and diffusion are fundamentally based and all parameters are physically significant.
2) The PSG method is suggested and validated for particle agglomeration due to collision and diffusion. Within a wide range of volume ratios, R_V, mass balance is satisfied and good matches are found. Because the accuracy of the PSG method increases with decreasing R_V, an R_V of 2.0 seems optimal.
3) PSG method needs only a small number of size groups to simulate particle agglomeration, and huge saving of memory storage and computational time is found by comparison with solving initial problem without losing mass balance and sacrificing the desired accuracy.
4) In addition to generate volume fraction and size distribution of precipitated particles, the PSG method is used to generate the PTT diagram.

Conclusions (grain growth)

1) In continuous casting, the grain growth model predicts grains approaching 50% of their final size by mold exit. The grains under 0.5mm oscillation marks are at least 10% larger than those on the slab surface due to local high temperature. Without precipitates, the grains are large enough to cause ductility problems

2) It is expected that the larger grains and lack of fine precipitates are likely the controlling factors to cause coarse grains and susceptibility to surface cracks beneath the oscillation marks. A program for coupling all the above models is necessary and important in future work

Acknowledgements

- Continuous Casting Consortium Members (ABB, Arcelor-Mittal, Baosteel, Corus, Delavan/Goodrich, LWB Refractories, Nucor, Nippon Steel, Postech, Steel Dynamics, ANSYS-Fluent)
- Prof. B. G. Thomas
- Other graduate students in CCC groups